

# The Outage Probability of a Finite Ad Hoc Network in Nakagami Fading

Don Torrieri and Matthew C. Valenti

**Abstract**—An ad hoc network with a finite spatial extent and number of nodes or mobiles is analyzed. The mobile locations may be drawn from any spatial distribution, and interference-avoidance protocols or protection against physical collisions among the mobiles may be modeled by placing an exclusion zone around each radio. The channel model accounts for the path loss, Nakagami fading, and shadowing of each received signal. The Nakagami  $m$ -parameter can vary among the mobiles, taking any positive value for each of the interference signals and any positive integer value for the desired signal. The analysis is governed by a new exact expression for the outage probability, defined to be the probability that the signal-to-interference-and-noise ratio (SINR) drops below a threshold, and is conditioned on the network geometry and shadowing factors, which have dynamics over much slower timescales than the fading. By averaging over many network and shadowing realizations, the average outage probability and transmission capacity are computed. Using the analysis, many aspects of the network performance are illuminated. For example, one can determine the influence of the choice of spreading factors, the effect of the receiver location within the finite network region, and the impact of both the fading parameters and the attenuation power laws.

**Index Terms**—Ad hoc networks, transmission capacity, Nakagami fading, spread spectrum.

## I. INTRODUCTION

An *ad hoc network* or peer-to-peer network comprises autonomous nodes or mobiles that communicate without a centralized control or assistance. Ad hoc networks, which have both commercial and military applications, possess no supporting infrastructure, fixed or mobile. In addition to being essential when a cellular infrastructure is not possible, ad hoc networks provide more robustness and flexibility in the presence of node or mobile failures than cellular networks. In this paper, we evaluate the performance of ad hoc networks of independent, identical mobiles that can operate simultaneously in the same spectral band.

In the quest for analytical tractability, most authors (e.g., [1] - [9] and the many references therein) assume the ad hoc network has an infinite number of mobiles spread over an infinite area and use the methods of stochastic geometry [10]. The locations of the mobiles at any time instant are

assumed to be spatially distributed as a Poisson point process, and performance measures are derived by averaging over the spatial distribution. When the network is finite, the Poisson point process is an inadequate model primarily because it allows an unbounded number of mobiles and does not account for the effects of the network boundary. However, this model is extremely useful because it enables authors to use Campbell's theorem [6], [10] to average over the possible network realizations and obtain tractable mathematical expressions that vastly simplify the performance analysis. Attempts to escape from the limitations of the Poisson point process [8] have involved restrictive assumptions such as a low density of mobiles [11] or operation in the high-reliability regime [12]. A universal assumption is identical fading models for all interference and reference signals, for instance Nakagami fading with a common Nakagami- $m$  parameter.

The analysis presented in this paper discards all previous assumptions about the spatial distribution of the network mobiles and identical fading. In this paper, the spatial extent of the network and number of mobiles are finite. Each mobile has an arbitrary location distribution with an allowance for the mobile's duty factor, shadowing, and possible exclusion zones. A new analysis is presented that computes the *exact* outage probability\* in the presence of Nakagami fading conditioned on the network geometry and shadowing. The Nakagami- $m$  parameter can vary among the mobiles, and the reference receiver need not be at the center of the network area.

The main result in this paper is a closed-form expression for the conditional outage probability at a reference receiver, which is conditioned on the location of the interferers and the realization of the shadowing. The expression averages over the fading, which has timescales much faster than that of the shadowing or node location. The channel from each mobile to the reference receiver may have its own distinct Nakagami- $m$  parameter, and the ability to vary the Nakagami- $m$  parameters can be used to model differing line-of-sight conditions between the reference receiver and each mobile. The outage probability in the presence of Nakagami- $m$  fading has been previously considered for interference-limited systems in [13] - [16]. None of these previous results accommodate thermal noise, and none are in closed form because they require the computation of derivatives [13], [14] or an infinite series [15], [16] for the most general case of interference with non-integer Nakagami- $m$  parameters. Furthermore, these previous works assume interference with fixed power and therefore do not consider the impact of the spatial model.

Paper approved by R. Schober, the Editor for Modulation and Signal Design of the IEEE Communications Society. Manuscript received Aug. 12, 2011; revised Mar. 26, 2012; accepted June 28, 2012.

M.C. Valenti's contribution was sponsored by the National Science Foundation under Award No. CNS-0750821 and by the United States Army Research Laboratory under Contract W911NF-10-0109.

D. Torrieri is with the US Army Research Laboratory, Adelphi, MD (email: dtorr@arl.army.mil).

M. C. Valenti is with West Virginia University, Morgantown, WV, U.S.A. (email: valenti@ieee.org).

Digital Object Identifier 10.1109/TCOMM.2012.01.XXXXXX

\*Outage probability is defined to be the probability that the signal-to-interference-and-noise ratio (SINR) drops below a threshold.

If unconditional outage probabilities are desired, then the conditional outage probability at the reference receiver can be averaged over the possible locations of the interfering mobiles and over the shadowing realizations. In limited cases, the averaging can be done analytically, and the Appendix derives the spatially averaged outage probability for the case that the reference receiver is at the center of an annular-shaped network, the interferers are uniformly distributed, and there is no shadowing. The unconditional outage probability can be computed for more general cases through the use of Monte Carlo simulation, which involves taking the numerical average over many network realizations, with the networks drawn according to the desired distributions that model the interferer locations and the shadowing. Because the fading does not need to be realized, such a simulation is extremely fast, with execution times that are competitive with the time required to compute analytical expressions when they are available.

A major advantage of our approach over others is that any spatial model can be analyzed, and the analysis can consider more than mere averages over interfering mobile locations. For instance, the probability that a network realization with specific mobile locations leads to a reference-receiver performance that fails to meet an outage constraint (the *network* outage probability) can be determined. Since our model allows realistic deployments, it can be incorporated into time-dependent random geometric graphs that capture the dynamic network status [17]. At each sampling instant, each mobile receiver has specified parameter values for the attenuation power law, the fading, and the shadowing from each signal source based on the terrain and mobile locations at that instant. The outage probabilities can be calculated by applying the closed-form equation presented in this paper. Our model alleviates many problems of other analytical models such as inability to handle arbitrarily located mobiles, simple link models with disc signal coverage, and no modeling of border effects.

The remainder of the paper is as follows. Section II presents a physical interference model of the network. Section III presents the derivation and description of the conditional outage probability. Some example outage-probability calculations are given in Section IV. The issues of spatial averaging and shadowing are discussed in Section V, while Section VI examines the effects of mobile density on both the outage probability and the transmission capacity. Conclusions are drawn in Section VII, while the Appendix derives a closed-form expression for the spatially averaged outage probability in the absence of shadowing when the reference receiver is at the center of an annular network of uniformly-distributed interferers.

## II. NETWORK MODEL

The network comprises  $M + 2$  mobiles that include a reference receiver, a desired or reference transmitter  $X_0$ , and  $M$  interfering mobiles  $X_1, \dots, X_M$ . The coordinate system is selected such that the reference receiver is at the origin. The variable  $X_i$  represents both the  $i^{\text{th}}$  mobile and its location, and  $\|X_i\|$  is the distance from the  $i^{\text{th}}$  mobile to the receiver. The mobiles can be located in any arbitrary two- or three-dimensional regions. Two-dimensional coordinates are conve-

niently represented by allowing  $X_i$  to assume a complex value, where the real component is the East-West coordinate and the imaginary component is the North-South coordinate.

Although the network area may have any arbitrary shape, we assume that it is a circular region of radius  $r_{net}$  in the subsequent examples. While the reference receiver is always located at the origin, the circular region encompassing the network does not need to be centered at the origin. Allowing the network to be centered at a coordinate other than the origin is equivalent to allowing the reference receiver to be located away from the center of the network. A circular *exclusion* zone of radius  $r_{ex}$  surrounds the reference receiver, and no interferers are permitted within the exclusion zone. The exclusion zone is a type of *guard zone*, and a nonzero  $r_{ex}$  may be used to model the effects of interference-avoidance protocols [18], [19], [20] or a prohibited zone to prevent physical collisions. When the reference receiver is located the center of the circular network region, the interferers are confined to an annulus with inner radius  $r_{ex}$  and outer radius  $r_{net}$ . For computational and analytical convenience, we normalize  $r_{net}$  so that  $r_{net} = 1$  (equivalently, the unit distance is defined to be  $r_{net}$ ).

Mobile  $X_i$  transmits a signal whose average received power in the absence of shadowing is  $P_i$  at a reference distance  $d_0$ . Typically, a common  $P_i = P_0$  is used for all mobiles since the unknown shadowing conditions make it difficult to adjust the power on a per-link basis. Signals may be spread with a direct-sequence waveform. Let  $G$  denote the *processing gain* or *spreading factor* of the direct-sequence spread-spectrum signal, which is equal to the increase in bandwidth ( $G = 1$  indicates no spreading).

In the ad hoc network, the multiple-access communications are asynchronous. Since there is no significant advantage to using short sequences, long spreading sequences are assumed and modeled as random binary sequences with chip duration  $T_c$ . The processing gain  $G$  directly reduces the interference power. The power of a multiple-access interference signal is further reduced by the chip factor  $h(\tau_o)$ , which is a function of the chip waveform and the timing offset  $\tau_o$  of the interference spreading sequence relative to that of the desired or reference signal. Since only timing offsets modulo- $T_c$  are relevant,  $0 \leq \tau_o < T_c$ . In a network of quadriphase direct-sequence systems, a multiple-access interference signal with power  $I$  before despreading is reduced after despreading to the power level  $Ih(\tau_o)/G$ , where [21], [22]

$$h(\tau_o) = \frac{1}{T_c^2} [R_\psi^2(\tau_o) + R_\psi^2(T_c - \tau_o)] \quad (1)$$

and  $R_\psi(\tau_o)$  is the partial autocorrelation for the normalized chip waveform. Thus, the interference power is effectively reduced by the factor  $G/h(\tau_o)$ . A *rectangular chip waveform* has  $R_\psi(\tau_o) = \tau_o$ , and hence

$$h(\tau_o) = 1 + 2 \left( \frac{\tau_o}{T_c} \right)^2 - 2 \left( \frac{\tau_o}{T_c} \right) \quad (2)$$

which implies that  $1/2 \leq h(\tau_o) \leq 1$ . If  $\tau_o$  is assumed to have a uniform distribution over  $[0, T_c]$ , then the expected value of  $h(\tau_o)$  is  $2/3$ . It is assumed henceforth that  $G/h(\tau_o)$  is a constant equal to  $G/h$  for all mobiles in the network.

After despreading, the power of  $X_i, i > 0$  (i.e.,  $X_i$  is an interferer), in the absence of shadowing at distance  $d_0$  is  $\tilde{P}_i = P_i(h/G)$ . For  $X_0$  (i.e., the reference transmitter), the power after despreading remains  $\tilde{P}_0 = P_0$ .

After despreading,  $X_i$ 's signal is received at the reference receiver with an instantaneous power

$$\rho_i = \tilde{P}_i g_i 10^{\xi_i/10} f(\|X_i\|) \quad (3)$$

where  $g_i$  is the power gain due to fading,  $\xi_i$  is a *shadowing factor*, and  $f(\cdot)$  is a path-loss function. The  $\{g_i\}$  are independent identically distributed (i.i.d.) and unit-mean with  $g_i = a_i^2$ , where  $a_i$  is Nakagami with parameter  $m_i$ . In Rayleigh fading,  $m_i = 1$  for all  $i$ , and the  $\{g_i\}$  are exponentially distributed. In the presence of log-normal shadowing, the  $\{\xi_i\}$  are i.i.d. zero-mean Gaussian with variance  $\sigma_s^2$ . In the absence of shadowing,  $\xi_i = 0$ . For  $d \geq d_0$ , the path-loss function is expressed as the attenuation power law

$$f(d) = \left(\frac{d}{d_0}\right)^{-\alpha} \quad (4)$$

where  $\alpha \geq 2$  is the attenuation power-law exponent, and it is assumed that  $d_0$  is sufficiently large that the signals are in the far field.

It is assumed that the  $\{g_i\}$  remain fixed for the duration of a time interval, but vary independently from interval to interval (block fading). With probability  $p_i$ , the  $i^{\text{th}}$  interferer transmits in the same time interval as the reference signal. The *activity probability*  $\{p_i\}$  can be used to model voice-activity factors or controlled silence. Although the  $\{p_i\}$  need not be the same, it is assumed that they are identical in the subsequent examples.

The instantaneous SINR at the receiver is

$$\gamma = \frac{\rho_0}{\mathcal{N} + \sum_{i=1}^M I_i \rho_i} \quad (5)$$

where  $\mathcal{N}$  is the noise power and  $I_i$  is a Bernoulli variable with probability  $P[I_i = 1] = p_i$  and  $P[I_i = 0] = 1 - p_i$ . Substituting (3) and (4) into (5) yields

$$\begin{aligned} \gamma &= \frac{P_0 g_0 10^{\xi_0/10} \|X_0\|^{-\alpha}}{\frac{\mathcal{N}}{d_0^\alpha} + \sum_{i=1}^M I_i \tilde{P}_i g_i 10^{\xi_i/10} \|X_i\|^{-\alpha}} \\ &= \frac{g_0 \Omega_0}{\Gamma^{-1} + \sum_{i=1}^M I_i g_i \Omega_i} \end{aligned} \quad (6)$$

where  $\Gamma = d_0^\alpha P_0 / \mathcal{N}$  is the signal-to-noise ratio (SNR) when the reference transmitter is at unit distance and fading and shadowing are absent, and

$$\Omega_i = \begin{cases} 10^{\xi_0/10} \|X_0\|^{-\alpha} & i = 0 \\ \frac{h P_i}{G P_0} 10^{\xi_i/10} \|X_i\|^{-\alpha} & i \geq 1 \end{cases} \quad (7)$$

is the normalized received power due to  $X_i$ .

### III. OUTAGE PROBABILITY

Let  $\Omega = [\Omega_0, \dots, \Omega_M]$  represent the set of normalized powers given by (7). An *outage* occurs when the SINR  $\gamma$  falls below an SINR threshold  $\beta$ , where  $\gamma$  is given for the particular  $\Omega$  by (6). It follows that the outage probability  $\epsilon$  for the given  $\Omega$  is

$$\epsilon = P[\gamma \leq \beta | \Omega]. \quad (8)$$

Because it is conditioned on  $\Omega$ , the outage probability is conditioned on the network geometry and shadowing factors, which have dynamics over timescales that are much slower than the fading. When conditioned on the fading and interference, the channel may be assumed to be AWGN, and the capacity  $C(\gamma)$  of the link conditioned on  $\Omega$  is a function of  $\gamma$ . The theoretically ideal SINR threshold may be found by inverting the capacity function for a given transmission rate  $R$ , i.e.,  $\beta = C^{-1}(R)$ .

Substituting (6) into (8), and rearranging yields

$$\epsilon = P\left[\beta^{-1} g_0 \Omega_0 - \sum_{i=1}^M I_i g_i \Omega_i \leq \Gamma^{-1} \mid \Omega\right]. \quad (9)$$

By defining

$$S = \beta^{-1} g_0 \Omega_0, \quad Y_i = I_i g_i \Omega_i \quad (10)$$

$$Z = S - \sum_{i=1}^M Y_i \quad (11)$$

the outage probability may be expressed as

$$\epsilon = P[Z \leq \Gamma^{-1} | \Omega] = F_Z(\Gamma^{-1} | \Omega) \quad (12)$$

which is the cumulative distribution function (cdf) of  $Z$  conditioned on  $\Omega$  and evaluated at  $\Gamma^{-1}$ .

Define  $\bar{F}_Z(z) = 1 - F_Z$  to be the complementary cdf of  $Z$ . Conditioned on  $\Omega$ , the complementary cdf of  $Z$  is

$$\begin{aligned} \bar{F}_Z(z | \Omega) &= P[Z > z | \Omega] = P\left[S > z + \sum_{i=1}^M Y_i \mid \Omega\right] \\ &= \int_{\mathbb{R}^M} \dots \int \left[ \int_{z + \sum y_i}^{\infty} f_S(s) ds \right] f_{\mathbf{Y}}(\mathbf{y}) d\mathbf{y} \end{aligned} \quad (13)$$

where  $f_{\mathbf{Y}}(\mathbf{y})$  is the joint probability density function (pdf) of the vector  $(Y_1, \dots, Y_M)$ , the pdf of the gamma-distributed  $S$  with Nakagami parameter  $m_0$  is

$$f_S(s) = \frac{\left(\frac{\beta m_0}{\Omega_0}\right)^{m_0}}{(m_0 - 1)!} s^{m_0 - 1} \exp\left\{-\frac{\beta m_0 s}{\Omega_0}\right\} \quad (14)$$

for  $s \geq 0$ , and the outer integral is over  $M$ -dimensional space.

Successive integration by parts and the assumption that  $m_0$  is a positive integer yield the solution to the inner integral:

$$\begin{aligned} \int_{z + \sum y_i}^{\infty} f_S(s) ds &= \exp\left\{-\frac{\beta m_0}{\Omega_0}(z + \sum y_i)\right\} \\ &\times \sum_{s=0}^{m_0-1} \frac{1}{s!} \left[\frac{\beta m_0}{\Omega_0}(z + \sum y_i)\right]^s \end{aligned} \quad (15)$$

Defining  $\beta_0 = \beta m_0 / \Omega_0$ , and substituting (15) into (13) yields

$$\begin{aligned} \bar{F}_Z(z|\Omega) &= e^{-\beta_0 z} \sum_{s=0}^{m_0-1} \frac{(\beta_0 z)^s}{s!} \\ &\times \int \dots \int_{\mathbb{R}^M} e^{-\beta_0 \sum y_i} \left(1 + z^{-1} \sum_{i=1}^M y_i\right)^s f_{\mathbf{Y}}(\mathbf{y}) d\mathbf{y}. \end{aligned} \quad (16)$$

Since  $s$  is a positive integer, the binomial theorem indicates that

$$\left(1 + z^{-1} \sum_{i=1}^M y_i\right)^s = \sum_{t=0}^s \binom{s}{t} z^{-t} \left(\sum_{i=1}^M y_i\right)^t. \quad (17)$$

A multinomial expansion yields

$$\left(\sum_{i=1}^M y_i\right)^t = t! \sum_{\substack{\ell_i \geq 0 \\ \sum_{i=0}^M \ell_i = t}} \left(\prod_{i=1}^M \frac{y_i^{\ell_i}}{\ell_i!}\right). \quad (18)$$

where the summation on the right-hand side is over all sets of indices that sum to  $t$ . Substituting (17) and (18) into (16), we obtain

$$\begin{aligned} \bar{F}_Z(z|\Omega) &= e^{-\beta_0 z} \sum_{s=0}^{m_0-1} \frac{(\beta_0 z)^s}{s!} \sum_{t=0}^s \binom{s}{t} z^{-t} t! \\ &\times \sum_{\substack{\ell_i \geq 0 \\ \sum_{i=0}^M \ell_i = t}} \int \dots \int_{\mathbb{R}^M} \left(\prod_{i=1}^M e^{-\beta_0 y_i} \frac{y_i^{\ell_i}}{\ell_i!}\right) f_{\mathbf{Y}}(\mathbf{y}) d\mathbf{y}. \end{aligned} \quad (19)$$

Using the fact that the  $\{Y_i\}$  are nonnegative and assuming that the interfering channels fade independently,

$$\begin{aligned} \bar{F}_Z(z|\Omega) &= e^{-\beta_0 z} \sum_{s=0}^{m_0-1} \frac{(\beta_0 z)^s}{s!} \sum_{t=0}^s \binom{s}{t} z^{-t} t! \\ &\times \sum_{\substack{\ell_i \geq 0 \\ \sum_{i=0}^M \ell_i = t}} \prod_{i=1}^M \int_0^\infty \frac{y_i^{\ell_i}}{\ell_i!} e^{-\beta_0 y_i} f_{Y_i}(y_i) dy_i. \end{aligned} \quad (20)$$

Taking into account the Nakagami fading and the activity probability  $p_i$ , the pdf of  $f_{Y_i}(y)$  is

$$\begin{aligned} f_{Y_i}(y) &= (1 - p_i) \delta(y) \\ &+ p_i \left(\frac{m_i}{\Omega_i}\right)^{m_i} \frac{1}{\Gamma(m_i)} y^{m_i-1} e^{-y m_i / \Omega_i} u(y) \end{aligned} \quad (21)$$

where  $u(y)$  is the unit-step function, and  $\delta(y)$  is the Dirac delta function. Substituting this pdf, the integral in (20) is

$$\begin{aligned} \int_0^\infty \frac{y_i^{\ell_i}}{\ell_i!} e^{-\beta_0 y_i} f_{Y_i}(y_i) dy_i &= (1 - p_i) \delta_{\ell_i} \\ &+ \left(\frac{p_i \Gamma(\ell_i + m_i)}{\ell_i! \Gamma(m_i)}\right) \left(\frac{\Omega_i}{m_i}\right)^{\ell_i} \left(\beta_0 \frac{\Omega_i}{m_i} + 1\right)^{-(m_i + \ell_i)} \end{aligned} \quad (22)$$

where  $\delta_\ell$  is the Kronecker delta function, equal to 1 when  $\ell = 0$ , and zero otherwise. Substituting (22) into (20) and using

$$\binom{s}{t} \binom{t!}{s!} = \binom{s!}{t!(s-t)!} \binom{t!}{s!} = \frac{1}{(s-t)!} \quad (23)$$

gives

$$\begin{aligned} \bar{F}_Z(z|\Omega) &= e^{-\beta_0 z} \sum_{s=0}^{m_0-1} (\beta_0 z)^s \sum_{t=0}^s \frac{z^{-t}}{(s-t)!} \\ &\times \sum_{\substack{\ell_i \geq 0 \\ \sum_{i=0}^M \ell_i = t}} \prod_{i=1}^M \left[ (1 - p_i) \delta_{\ell_i} + \frac{p_i \Gamma(\ell_i + m_i) \left(\frac{\Omega_i}{m_i}\right)^{\ell_i}}{\ell_i! \Gamma(m_i) \left(\beta_0 \frac{\Omega_i}{m_i} + 1\right)^{(m_i + \ell_i)}} \right]. \end{aligned} \quad (24)$$

This equation may be written as

$$\bar{F}_Z(z|\Omega) = e^{-\beta_0 z} \sum_{s=0}^{m_0-1} (\beta_0 z)^s \sum_{t=0}^s \frac{z^{-t} H_t(\Psi)}{(s-t)!} \quad (25)$$

where

$$\Psi_i = \left(\beta_0 \frac{\Omega_i}{m_i} + 1\right)^{-1} \quad \text{for } i = \{1, \dots, M\}, \quad (26)$$

$$H_t(\Psi) = \sum_{\substack{\ell_i \geq 0 \\ \sum_{i=0}^M \ell_i = t}} \prod_{i=1}^M G_{\ell_i}(\Psi_i), \quad (27)$$

$$G_\ell(\Psi_i) = \begin{cases} 1 - p_i (1 - \Psi_i^{m_i}) & \text{for } \ell = 0 \\ \frac{p_i \Gamma(\ell + m_i)}{\ell! \Gamma(m_i)} \left(\frac{\Omega_i}{m_i}\right)^\ell \Psi_i^{m_i + \ell} & \text{for } \ell > 0. \end{cases} \quad (28)$$

Equation (27) may be efficiently computed as follows. For each possible  $t = \{0, \dots, m_0 - 1\}$ , precompute a matrix  $\mathcal{I}_t$  whose rows contain all sets of non-negative indices  $\{\ell_1, \dots, \ell_M\}$  that sum to  $t$ . There will be

$$\binom{t + M - 1}{t} \quad (29)$$

rows and  $M$  columns in  $\mathcal{I}_t$ . The  $\mathcal{I}_t$ 's may be reused anytime the same  $M$  is considered. Compute a row vector  $\Psi$  containing the  $\Psi_i$ . For each possible  $\ell = \{0, \dots, m_0 - 1\}$ , compute (28) using  $\Psi$  and place the resulting row into an  $m_0 \times M$  matrix  $\mathbf{G}$ . Each term of (27) can be found by using the corresponding row from  $\mathcal{I}_t$  as an index into  $\mathbf{G}$ . Taking the product along the length of the resulting row vector gives the corresponding term of the summation. More generally, the entire  $\mathcal{I}_t$  matrix can be used to index  $\mathbf{G}$ . To be consistent with matrix-based languages, such as Matlab, denote the result of the operation as  $\mathbf{G}(\mathcal{I}_t)$ . Taking the product along the rows of  $\mathbf{G}(\mathcal{I}_t)$  and then the sum down the resulting column gives (27).

#### IV. EXAMPLES

Consider the network topology shown in the upper right corner of Fig. 1. The reference receiver is at the center of the network, and  $M = 28$  interferers are within an annular region with inner radius  $r_{ex} = 0.05$  and outer radius  $r_{net} = 1$ . An exclusion zone of radius  $r_{ex}$  surrounds each mobile, and interfering mobiles are uniformly distributed throughout the network area outside of the exclusion zones. Mobiles are placed successively according to a *uniform clustering* model as follows. Let  $X_i = r_i e^{j\theta_i}$  represent the location of the  $i^{\text{th}}$  mobile. A pair of independent random variables  $(y_i, z_i)$  is selected from the uniform distribution over  $[0, 1]$ . From

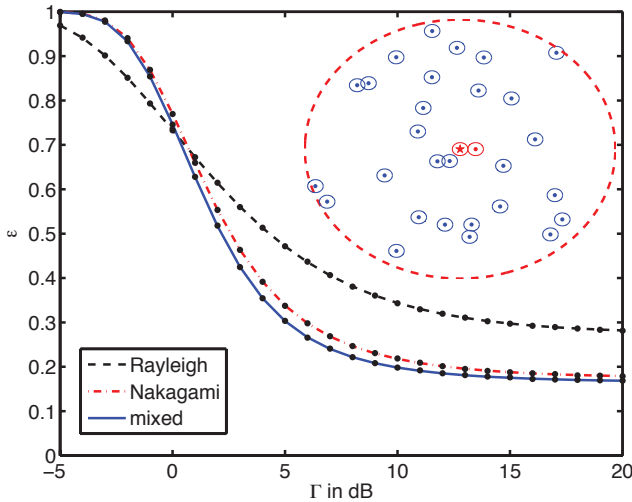


Fig. 1. An example network, which is drawn according to the uniform clustering model, is shown in the upper right portion of the figure. The reference receiver (indicated by the  $\star$ ) is placed at the origin, and the corresponding reference transmitter is located to its right (indicated by the  $\bullet$  to the right of the receiver).  $M = 28$  interferers (indicated by the  $\bullet$ ) are placed at random within the dashed circle. An exclusion zone surrounds each mobile (indicated by solid circles surrounding the mobiles). The figure also shows the outage probability as a function of SNR  $\Gamma$ , conditioned on the pictured network topology. Performance is shown for three fading models without spreading or shadowing. Analytical expressions are plotted by lines while dots represent simulation results (with one million trials per point).

these variables, the location is initially selected according to a uniform spatial distribution over a disk with radius  $r_{net}$  by setting  $r_i = \sqrt{y_i}r_{net}$  and  $\theta_i = 2\pi z_i$ . If the corresponding  $X_i$  falls within an exclusion zone of one of the  $i - 1$  previous mobile locations, then a new random location is assigned to the  $i^{th}$  mobile as many times as necessary until it falls outside any exclusion zone.

Once the mobile locations  $\{X_i\}$  are realized, the  $\{\Omega_i\}$  are determined by assuming an attenuation power-law exponent  $\alpha = 3.5$ , a common transmit power  $P_i = P$  for all  $i$ , no shadowing, and that the reference transmitter is at distance  $\|X_0\| = 0.1$  from the reference receiver. For all results given in this paper, the value of  $p_i = 0.5$  for all  $i$ , and the SINR threshold is  $\beta = 0$  dB, which corresponds to the unconstrained AWGN capacity limit for a rate-1 channel code and complex inputs.

**Example #1.** Suppose that spread-spectrum modulation is not used ( $G = h = 1$ ) and that all signals undergo Rayleigh fading. Then,  $m_i = 1$  for all  $i$ ,  $\beta_0 = \beta/\Omega_0 = \beta\|X_0\|^\alpha$ ,  $\Omega_i = \|X_i\|^{-\alpha}$ , and (25) specializes to

$$\bar{F}_Z(z|\Omega) = e^{-\beta_0 z} \prod_{i=1}^M \frac{1 + \beta_0(1 - p_i)\Omega_i}{1 + \beta_0\Omega_i}. \quad (30)$$

The outage probability can thus be readily found for any given realization of  $\Omega$ . The outage probability, found by evaluating (30) at  $z = \Gamma^{-1}$ , is shown along with the spatial locations of the mobiles in Fig. 1. Also shown is the outage probability generated by simulation, which involves randomly generating the mobile locations and the exponentially distributed power gains  $g_0, \dots, g_M$ . As can be seen in the figure, the analytical and simulation results coincide, which is to be expected because (30) is exact. Any discrepancy between the curves

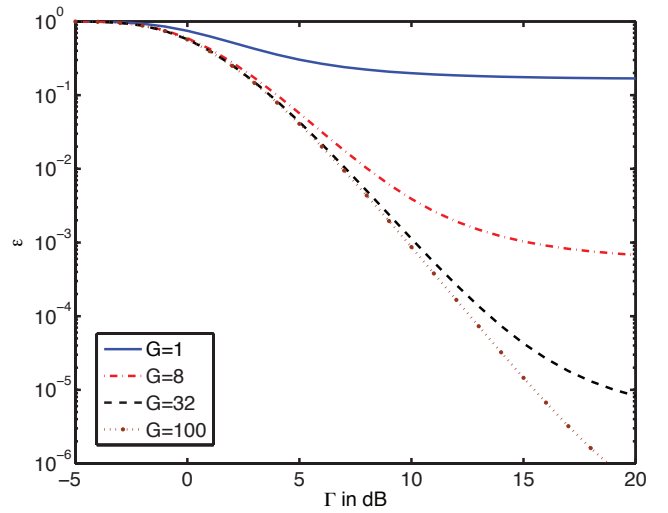


Fig. 2. Outage probability as a function of SNR  $\Gamma$ , conditioned on the network shown in Fig. 1 with the mixed-fading model. Performance is shown both with and without spreading for several values of processing gain ( $G$ ).

can be attributed to the finite number of Monte Carlo trials (one million trials were executed per SNR point).

**Example #2.** Now suppose that the link between the source and receiver undergoes Nakagami fading with parameter  $m_0 = 4$ . The outage probability, found using (25) through (28), is also plotted in Fig. 1. The figure shows two choices for the Nakagami parameter of the interferers:  $m_i = 1$  and  $m_i = 4$ ,  $i = 1, 2, \dots, M$ . The  $m_i = 4$  case, denoted by “Nakagami” in the figure legend, represents the situation where the reference transmitter and interferers are equally visible to the receiver. The  $m_i = 1$  case, denoted by “mixed” in the figure legend, represents a more typical situation where the interferers are not in the line-of-sight. As with the previous example, the analytical curves are verified by simulations involving one million Monte Carlo trials per SNR point.

**Example #3.** The outage probabilities of examples #1 and #2 are very high. One way to reduce the outage probability is to use spread spectrum. Suppose that direct-sequence spread spectrum is used with a processing gain of  $G$  and  $h = 2/3$ . In Fig. 2, the outage probability is shown for direct-sequence networks using three different processing gains as well as for an unspread network ( $G = h = 1$ ). A mixed fading model ( $m_0 = 4$  and  $m_i = 1$  for  $i \geq 1$ ) is used. From this plot, a dramatic reduction in outage probability when using direct-sequence spreading can be observed.

## V. SPATIAL AVERAGING

Because it is conditioned on  $\Omega$ , the outage probability will vary from one network realization to the next. The variability in outage probability is illustrated in Fig. 3, which shows the outage probability for ten different network realizations. One of the networks is the one shown in Fig. 1 while the other nine networks were each realized in the same manner; i.e., with  $M = 28$  interferers drawn from a uniform clustering process with  $r_{ex} = 0.05$  and  $r_{net} = 1$  and the reference transmitter placed at distance  $\|X_0\| = 0.1$  from the reference receiver. The same set of parameters ( $\alpha$ ,  $\beta$ ,  $p_i$ ,  $P_i$ , and  $m_i$ ) used to generate the mixed-fading results of Example #2 were

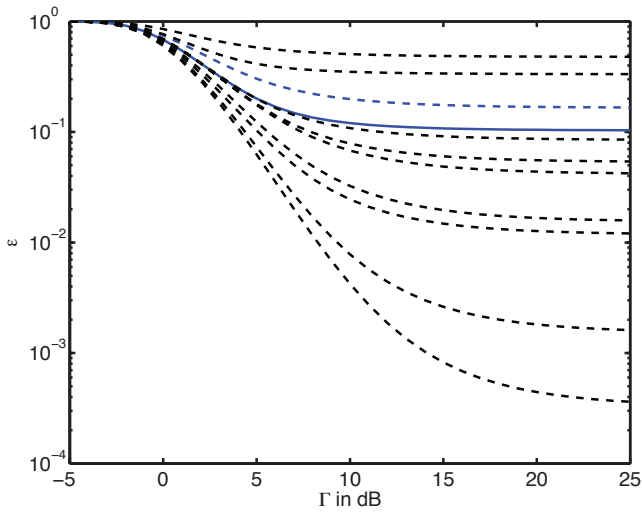


Fig. 3. Outage probability conditioned on several different network realizations. A uniform clustering model is assumed with  $r_{net} = 1.0$ ,  $r_{ex} = 0.05$ ,  $M = 28$ , mixed fading,  $\alpha = 3.5$ , and no spreading. Ten network realizations were drawn, and the conditional outage probabilities are indicated by dashed lines. The average outage probability over 10,000 network realizations  $\bar{\epsilon}$  is shown by the solid line.

again used, and signals were not spread. From the figure, it can be seen that the outage probabilities of different network realizations can vary dramatically.

In addition to the location of the interferers,  $\Omega$  depends on the realization of the shadowing. The shadowing factors  $\{\xi_i\}$  can have any arbitrary distribution and need not be the same for all  $i$ . In subsequent examples, log-normal shadowing is assumed, and the shadow factors are i.i.d. Gaussian with a standard deviation  $\sigma_s$  and zero mean.

The conditioning on  $\Omega$  can be removed by marginalizing  $\bar{F}_Z(z|\Omega)$  with respect to the spatial distribution of the network and the distribution of the shadowing. This can be done analytically under certain limitations. For instance, with the reference receiver at the center of the network, a uniform spatial distribution, and no shadowing, the average outage probability can be found, as shown in the Appendix. For more general cases of interest, such as correlated spatial distributions (including uniform clustering processes and Matérn processes [8]) or the presence of shadowing, closed-form expressions are not readily available. However, the outage probability can be estimated through Monte Carlo simulation by generating a number of  $\Omega$ , computing the outage probability of each, and taking the average. Suppose that  $N$  networks are generated, and let  $\Omega = \Omega_i$  for the  $i^{th}$  network. Then the average outage probability may be found from the Monte Carlo estimate of the complementary cdf:

$$\bar{F}_Z(z) = \frac{1}{N} \sum_{i=1}^N \bar{F}_Z(z|\Omega_i). \quad (31)$$

The average outage probability is

$$\bar{\epsilon} = 1 - \bar{F}_Z(\Gamma^{-1}). \quad (32)$$

As an example, the solid line in Fig. 3 shows the corresponding average outage probability averaged over  $N = 10,000$  network realizations.

TABLE I  
AVERAGE OUTAGE PROBABILITY WHEN THE RECEIVER IS AT THE CENTER OF THE NETWORK FOR VARIOUS VALUES OF  $M$ ,  $\alpha$ , AND  $G$  WITH UNIFORMLY DISTRIBUTED INTERFERERS AND NO SHADOWING. THE COLUMN MARKED  $\bar{\epsilon}_s$  IS THE AVERAGE OBTAINED THROUGH SIMULATION WHILE THE COLUMN MARKED  $\bar{\epsilon}_t$  IS THE THEORETICAL VALUE.

$M$	$\alpha$	$G$	$\bar{\epsilon}_s$	$\bar{\epsilon}_t$
30	3	1	$1.730 \times 10^{-1}$	$1.711 \times 10^{-1}$
		32	$1.874 \times 10^{-3}$	$1.906 \times 10^{-3}$
	4	1	$1.303 \times 10^{-1}$	$1.290 \times 10^{-1}$
		32	$3.010 \times 10^{-3}$	$3.118 \times 10^{-3}$
60	3	1	$3.572 \times 10^{-1}$	$3.624 \times 10^{-1}$
		32	$3.130 \times 10^{-3}$	$3.229 \times 10^{-3}$
	4	1	$2.518 \times 10^{-1}$	$2.574 \times 10^{-1}$
		32	$5.429 \times 10^{-3}$	$5.671 \times 10^{-3}$

Table I compares the spatially averaged outage probability obtained using the theoretical expression from the Appendix against the corresponding value obtained by performing a Monte Carlo averaging over  $N = 10,000$  network realizations. For the results shown in Table I, the network radius is normalized to  $r_{net} = 1$ , the reference transmitter placed at distance  $\|X_0\| = 0.1$ , the SINR threshold set to  $\beta = 0$  dB, and the activity factor set to  $p_i = 0.5$ . An unshadowed mixed-fading channel was used with SNR set to  $\Gamma = 10$  dB. An exclusion zone of radius  $r_{ex} = 0.05$  surrounds just the reference receiver. Exclusion zones are not placed around the interferers or reference transmitter, which ensures that the interferers are independently placed according to a uniform distribution over the annulus of inner radius  $r_{ex}$  and outer radius  $r_{net}$ . Table I shows the average outage probability for  $M = \{30, 60\}$ ,  $\alpha = \{3, 4\}$ , and  $G = \{1, 32\}$ . As can be seen, there is a good agreement between the theoretical values and those obtained by simulating the interferer locations. The Monte Carlo approach has an uncertainty that decreases with increasing  $N$ , and is an effective approach to handle those cases that cannot be solved with the analytical expression of the Appendix.

Although the spatially averaged outage probability  $\bar{\epsilon}$  provides some insight into the average network behavior, it does not capture the dynamics of the spatial distribution. A more useful metric for quantifying the spatial variability is the probability that the conditional outage probability  $\epsilon$  is either above or below a threshold  $\epsilon_T$ . In particular  $P[\epsilon > \epsilon_T]$  represents the fraction of network realizations that fail to meet a minimum required outage probability at the reference receiver and can be construed as a *network* outage probability. The complement of the network outage probability  $P[\epsilon \leq \epsilon_T]$  is the cdf of  $\epsilon$ :  $F_\epsilon(\epsilon_T)$ . This probability is shown in Fig. 4 for the three fading models without spreading, and for the mixed-fading model with spreading. For each curve, the SNR is  $\Gamma = 10$  dB and the system parameters are the same as the corresponding Examples given in Section IV. Each curve was generated by drawing  $N = 10,000$  networks using the same spatial model used to generate the Examples; i.e., with  $M = 28$  interferers drawn from a uniform clustering process with  $r_{ex} = 0.05$ ,  $r_{net} = 1$ , and no shadowing. For each network, the outage probability was computed and compared against the threshold  $\epsilon_T$ . The curves show the fraction of networks whose  $\epsilon$  does not exceed the threshold. Note that the

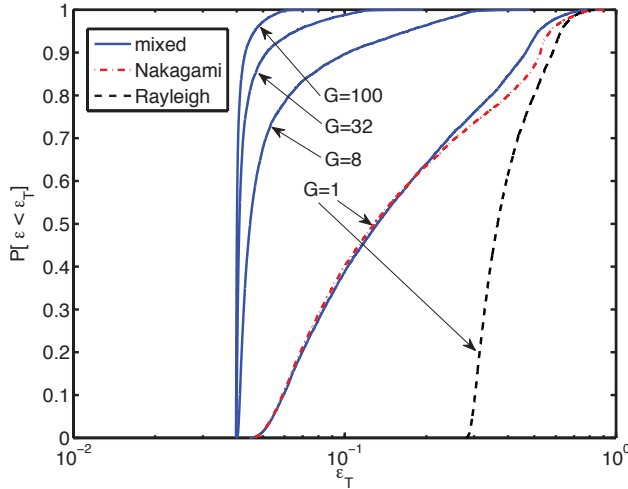


Fig. 4. Probability that the conditional outage probability  $\epsilon$  is below the threshold outage probability  $\epsilon_T$  in a network with  $r_{net} = 1.0$ ,  $r_{ex} = 0.05$ ,  $M = 28$ , and  $\Gamma = 5$  dB.  $N = 10,000$  network realizations were drawn to produce the figure. Results are shown for the three fading models without spreading ( $G = 1$ ) and for the mixed-fading model with spreading ( $G = \{8, 32, 100\}$ ).

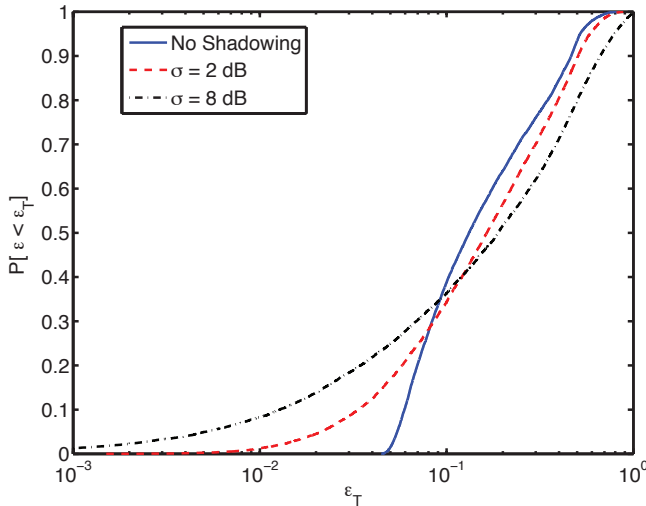


Fig. 5. Probability that the conditional outage probability  $\epsilon$  is below the threshold outage probability  $\epsilon_T$  in a network with  $r_{ex} = 0.05$ ,  $r_{net} = 1.0$ ,  $M = 28$ ,  $\Gamma = 5$  dB, mixed fading, and no spreading ( $G = 1$ ).  $N = 10,000$  network realizations were drawn to produce the figure. Curves shown for no shadowing, and shadowing with two values of  $\sigma_s$ .

curves become steeper with increasing  $G$ , which shows that spreading has the effect of making performance less sensitive to the particular network topology.

Shadowing can be incorporated into the model by simply drawing an appropriate set of independent shadowing factors  $\{\xi_i\}$  for each network realization and using them to compute the  $\{\Omega_i\}$  according to (7). In Fig. 5, shadowing was applied to the same set of  $N = 10,000$  networks used to generate Fig. 4. Two standard deviations were considered for the log-normal shadowing:  $\sigma_s = 2$  dB and  $\sigma_s = 8$  dB, and again  $\alpha = 3.5$ . For each shadowed network realization, the outage probability was computed for the mixed-fading model without spreading ( $G = 1$ ). All other parameter values are the same ones used to produce Fig. 4. The figure shows  $P[\epsilon \leq \epsilon_T]$ , and the no-shadowing case is again shown for reference.

TABLE II  
AVERAGE OUTAGE PROBABILITY WHEN THE RECEIVER IS AT THE CENTER ( $\bar{\epsilon}_c$ ) AND ON THE PERIMETER ( $\bar{\epsilon}_p$ ) OF THE NETWORK FOR VARIOUS  $M$ ,  $\alpha$ ,  $G$ , AND  $\sigma_s$ .

Parameters				Outage probabilities		
$M$	$\alpha$	$G$	$\sigma_s$	$\bar{\epsilon}_c$	$\bar{\epsilon}_p$	
30	3	1	0	0.1528	0.0608	
			8	0.2102	0.0940	
		32	0	0.0017	0.0012	
			8	0.0112	0.0085	
		4	1	0	0.1113	0.0459
			8	0.1410	0.0636	
	60	3	1	0	0.3395	0.1328
				8	0.4102	0.1892
			32	0	0.0030	0.0017
		8		0.0163	0.0107	
		4	1	0	0.2333	0.0954
				8	0.2769	0.1247
32	0		0.0052	0.0027		
			8	0.0184	0.0117	

As can be seen from the figure, the presence of shadowing and increases in  $\sigma_s$  increase the variability of the conditional outage probability, as indicated by the reduced slope of the cdf curves. Interestingly, shadowing does not significantly alter the average outage probability in this example. For low thresholds, such as  $\epsilon_T < 0.1$ , performance is actually better with shadowing than without. This behavior is presumably due to the fact that, in shadowing, the reference signal power will sometimes be much higher than without shadowing.

In a finite network, the average outage probability depends on the location of the reference receiver. Rather than leaving the reference receiver at the origin, Table II explores the change in performance when the reference receiver moves from the center of the radius- $r_{net}$  circular network to the perimeter of the network. When the reference receiver is at the perimeter of the network, the circular network region is centered at coordinate  $-r_{net}$ . The SNR was set to  $\Gamma = 10$  dB, a mixed-fading channel model was assumed, and other parameter values are the same ones used to produce Fig. 5; i.e.,  $r_{ex} = 0.05$ ,  $r_{net} = 1$ ,  $\beta = 0$  dB, and  $p_i = 0.5$ . The interferers were placed according to the uniform clustering model and the reference transmitter was placed at distance  $\|X_0\| = 0.1$  from the reference receiver. For each set of values of the parameters  $G$ ,  $\alpha$ ,  $\sigma_s$ , and  $M$ , the outage probability at the network center  $\bar{\epsilon}_c$  and at the network perimeter  $\bar{\epsilon}_p$  were computed by averaging over  $N = 10,000$  realizations of mobile placement and shadowing. Two values of each parameter were considered:  $G = \{1, 32\}$ ,  $\alpha = \{3, 4\}$ ,  $\sigma_s = \{0, 8\}$ ,  $M = \{30, 60\}$ . The table indicates that  $\bar{\epsilon}_p$  is considerably less than  $\bar{\epsilon}_c$  in the finite network, which cannot be predicted by the traditional infinite-network model. This reduction in outage probability is more significant for the unspread network, and is less pronounced with increasing  $G$ . Both  $\bar{\epsilon}_p$  and  $\bar{\epsilon}_c$  increase as  $M$  and  $\sigma_s$  increase and  $G$  decreases.

As  $\alpha$  increases, both  $\bar{\epsilon}_p$  and  $\bar{\epsilon}_c$  increase when  $G = 32$ , but decrease when  $G = 1$ . This difference occurs because spread-spectrum systems are less susceptible to the near-far problem than unspread ones. The increase in  $\alpha$  is not enough to cause a significant increase in the already high outage probability for

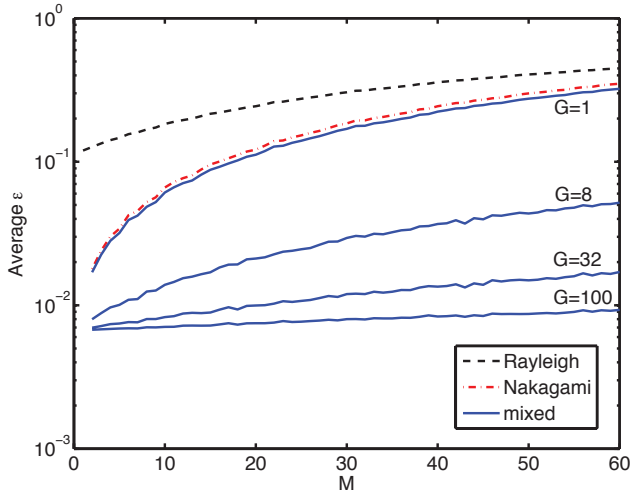


Fig. 6. Average outage probability as a function of  $M$  for SNR  $\Gamma = 10$  dB and log-normal shadowing with  $\sigma_s = 8$  dB. Results are shown for the three fading models without spreading ( $G = 1$ ) and for the mixed-fading model with spreading ( $G = \{8, 32, 100\}$ ).

unspread systems in those realizations with interferers close enough to the reference receiver to cause a near-far problem. In the same realizations, the less susceptible spread-spectrum systems do experience a significantly increased outage probability.

## VI. NUMBER OF INTERFERERS AND TRANSMISSION CAPACITY

Fig. 6 shows the outage probability averaged over 10,000 networks as a function of the number of interferers  $M$  in the presence of log-normal shadowing with standard-deviation  $\sigma_s = 8$  dB. A uniform-clustering network model is again assumed with  $r_{ex} = 0.05$  and  $r_{net} = 1$ , and the reference receiver is at the center of the network ( $r = 0$ ). The SNR is  $\Gamma = 10$  dB and the parameters  $\alpha = 3.5$ ,  $p_i = 0.5$ , and  $\beta = 0$  dB are again used. Results are shown for the unspread network and the three channel models of Examples #1 and #2, as well as for the mixed-fading channel model and three spreading factors  $G = \{8, 32, 100\}$ . From the curves, it can be observed that performance improves with increasing  $G$ , and that higher values of  $G$  reduce the sensitivity to an increased density of interfering mobiles. Both of these effects are attributable to the improved interference suppression as the processing gain increases.

A trade-off can be seen in Fig. 6. As  $M$  increases, the performance of each link degrades, yet there will be more simultaneous transmissions supported by the network. This trade-off can be quantified by the *transmission capacity*, which represents the network throughput per unit area [1]. It can be found by multiplying network density  $\lambda$ , which is the number of mobiles per unit area, by the rate that bits are successfully transmitted over the reference link:

$$\tau = \lambda(1 - \epsilon)b \quad (33)$$

where  $b$  is the per-link throughput in the absence of an outage, in units of bps, and the factor  $(1 - \epsilon)$  ensures that only successful transmissions are counted.

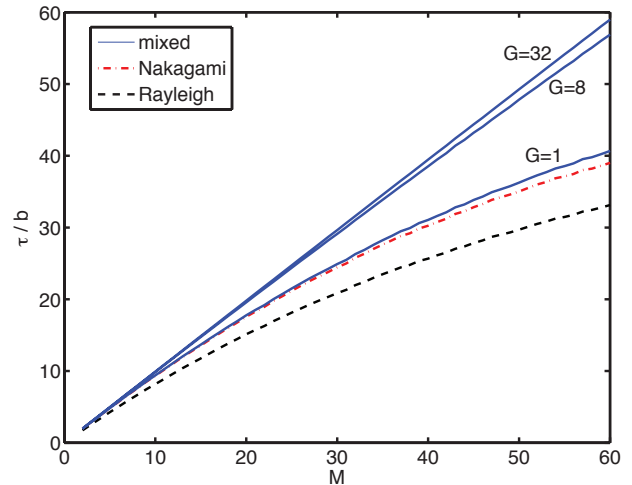


Fig. 7. Normalized transmission capacity as a function of  $M$  for SNR  $\Gamma = 10$  dB and log-normal shadowing with  $\sigma_s = 8$  dB. Results are shown for the three fading models without spreading ( $G = 1$ ) and for the mixed-fading model with spreading ( $G = \{8, 32\}$ ). The performance with  $G = 100$  is not shown and is slightly higher than it is for  $G = 32$ .

Fig. 7 shows the transmission capacity normalized by  $b$  as a function of  $M$  for the same cases shown in Fig. 6. As can be seen from the figure, spreading improves the transmission capacity due to the corresponding reduction in outage probability. The curves become steeper with increasing  $G$  reflecting the superior ability of spreading to cope with increasing network density, provided that enough bandwidth is available to support the spread-spectrum signaling.

## VII. CONCLUSION

A new and potent method for evaluating the performance of an ad hoc network has been presented. Since our model allows realistic deployments, it can be incorporated into time-dependent random geometric graphs that capture the dynamic network status. Factors modeled include a finite spatial extent and number of mobiles, any spatial distribution of the mobiles, the existence of exclusion zones, path-loss, Nakagami fading, and shadowing. The Nakagami  $m$ -parameter can vary among the mobiles provided that it is an integer for the reference transmitter. Using the analysis, many aspects of the network performance are illuminated. For example, one can determine the influence of the choice of the spreading factor, the effect of the receiver location within the finite network region, and the impact of the attenuation power law.

## APPENDIX

By averaging over  $\Omega_1 = \{\Omega_1, \dots, \Omega_M\}$ , the complementary cdf of  $Z$  is

$$\bar{F}_Z(z) = \int f_{\Omega}(\omega) \bar{F}_Z(z|\omega) d\omega \quad (34)$$

where  $f_{\Omega}(\omega)$  is the joint pdf of  $\Omega_1$ . Assuming that the  $\{\Omega_i\}$  are independent,

$$f_{\Omega}(\omega) = \prod_{i=1}^M f_{\Omega_i}(\omega_i) \quad (35)$$



$$\bar{F}_z(z) = e^{-\beta_0 z} \sum_{s=0}^{m_0-1} (\beta_0 z)^s \sum_{t=0}^s \frac{z^{-t}}{(s-t)!} \sum_{\substack{\ell_i \geq 0 \\ \sum_{i=0}^M \ell_i = t}} \prod_{i=1}^M \left[ (1-p_i) \delta_{\ell_i} + \frac{2p_i \Gamma(\ell_i + m_i)}{\alpha c_i^{2/\alpha} (r_{net}^2 - r_{ex}^2) (\ell_i!) \Gamma(m_i)} \int_{c_i r_{ex}^\alpha}^{c_i r_{net}^\alpha} \frac{x^{(\frac{2-\alpha}{\alpha})} \left(\frac{1}{m_i x}\right)^{\ell_i}}{\left(\frac{\beta_0}{m_i x} + 1\right)^{(m_i + \ell_i)}} dx \right] \quad (39)$$

$$\bar{F}_z(z) = e^{-\beta_0 z} \sum_{s=0}^{m_0-1} (\beta_0 z)^s \sum_{t=0}^s \frac{z^{-t}}{(s-t)!} \sum_{\substack{\ell_i \geq 0 \\ \sum_{i=0}^M \ell_i = t}} \prod_{i=1}^M \left[ (1-p_i) \delta_{\ell_i} + \frac{2p_i \Gamma(\ell_i + m_i) m_i^{m_i} [J(c_i r_{net}^\alpha) - J(c_i r_{ex}^\alpha)]}{\alpha c_i^{2/\alpha} (r_{net}^2 - r_{ex}^2) (\ell_i!) \Gamma(m_i) \beta_0^{(m_i + \ell_i)} \left(m_i + \frac{2}{\alpha}\right)} \right] \quad (44)$$

where  $f_{\Omega_i}(\omega_i)$  is the pdf of  $\Omega_i$ . Define  $\mathcal{U}_i = \Omega_i^{-1}$ ,  $i \geq 1$ , to be the *inverse* normalized power of the  $i^{th}$  interferer. Using (35) and the definition of  $\mathcal{U}_i$ , (34) may be expressed as

$$\bar{F}_z(z) = \int \left( \prod_{i=1}^M f_{\mathcal{U}_i}(x_i) \right) \bar{F}_z(z | \{x_1^{-1}, \dots, x_M^{-1}\}) dx. \quad (36)$$

If the location of interferer  $X_i$  is uniform within the annulus of inner radius  $r_{ex}$  and outer radius  $r_{net}$ , then its distance  $r_i = \|X_i\|$  from the origin has pdf

$$f_{r_i}(r) = \begin{cases} \frac{2r}{r_{net}^2 - r_{ex}^2} & \text{for } r_{ex} \leq r \leq r_{net} \\ 0 & \text{elsewhere.} \end{cases} \quad (37)$$

From the definition of  $\mathcal{U}_i$  and (7),  $\mathcal{U}_i = (G/h)(P_0/P_i)r_i^\alpha$ ,  $i \geq 1$ , in the absence of shadowing, and it follows that the pdf of  $\mathcal{U}_i$  is

$$f_{\mathcal{U}_i}(x) = \begin{cases} \frac{2x^{(\frac{2-\alpha}{\alpha})}}{\alpha c_i^{2/\alpha} (r_{net}^2 - r_{ex}^2)} & \text{for } c_i r_{ex}^\alpha \leq x \leq c_i r_{net}^\alpha \\ 0 & \text{elsewhere} \end{cases} \quad (38)$$

where  $c_i = (G/h)(P_0/P_i)$ . Substituting (25) and (38) into (36) and extracting factors from the integral that are independent of the variable of integration yields equation (39) at the top of the page, where  $\beta_0 = \beta m_0 \|X_0\|^\alpha$  in the absence of fading.

By factoring the denominator and splitting the integration interval, the integral in (39) is

$$\int_a^b \frac{x^{(\frac{2-\alpha}{\alpha})} \left(\frac{1}{m_i x}\right)^{\ell_i}}{\left(\frac{\beta_0}{m_i x} + 1\right)^{(m_i + \ell_i)}} dx = \frac{m_i^{m_i}}{\beta_0^{(m_i + \ell_i)}} [I(b) - I(a)] \quad (40)$$

where  $a = c_i r_{ex}^\alpha$ ,  $b = c_i r_{net}^\alpha$ , and

$$I(y) = \int_0^y x^{(m_i + \frac{2}{\alpha} - 1)} \left(1 + \frac{m_i x}{\beta_0}\right)^{-(m_i + \ell_i)} dx. \quad (41)$$

By performing the change of variable  $x = y\nu$ ,

$$\begin{aligned} I(y) &= \int_0^1 (y\nu)^{(m_i + \frac{2}{\alpha} - 1)} \left(1 + \frac{m_i y\nu}{\beta_0}\right)^{-(m_i + \ell_i)} y d\nu \\ &= y^{(m_i + \frac{2}{\alpha})} \int_0^1 \nu^{(m_i + \frac{2}{\alpha} - 1)} \left(1 + \frac{m_i y}{\beta_0} \nu\right)^{-(m_i + \ell_i)} d\nu \\ &= \frac{y^{(m_i + \frac{2}{\alpha})}}{(m_i + \frac{2}{\alpha})} {}_2F_1 \left( \left[ m_i + \ell_i, m_i + \frac{2}{\alpha} \right]; m_i + \frac{2}{\alpha} + 1; -\frac{m_i y}{\beta_0} \right) \end{aligned} \quad (42)$$

where  ${}_2F_1$  is the Gauss hypergeometric function, which has the integral representation:

$${}_2F_1([a, b]; c; x) = \frac{\Gamma(c)}{\Gamma(b)\Gamma(c-b)} \int_0^1 \nu^{b-1} (1-\nu)^{c-b-1} (1-x\nu)^{-a} d\nu \quad (43)$$

and  $c = b + 1$ ,  $\Gamma(c)/(\Gamma(b)\Gamma(c-b)) = b$ . The hypergeometric function can be represented by an infinite series if  $|x| < 1$  and is evaluated by analytical continuation if  $|x| \geq 1$  [23], [24]. The function is widely known and is implemented as a single function call in most mathematical programming languages, including Matlab. The complementary cdf of  $Z$  can be found by substituting (40) into (39), with the  $I(\cdot)$  function as defined in (42). The result is equation (44) at the top of the page, where

$$J(y) = {}_2F_1 \left( \left[ m_i + \ell_i, m_i + \frac{2}{\alpha} \right]; m_i + \frac{2}{\alpha} + 1; -\frac{m_i y}{\beta_0} \right) y^{m_i + \frac{2}{\alpha}} \quad (45)$$

## REFERENCES

- [1] S. Weber, J. G. Andrews, and N. Jindal, "An overview of the transmission capacity of wireless networks," *IEEE Trans. Commun.*, vol. 58, pp. 3593–3604, December 2010.
- [2] K. Gulati, B. L. Evans, J. G. Andrews and K. R. Tinsley, "Statistics of Co-Channel Interference in a Field of Poisson and Poisson-Poisson Clustered Interferers", *IEEE Trans. Signal Processing*, vol. 58, pp. 6207–6222, Dec. 2010.
- [3] E. Salbaroli and A. Zanella, "Interference analysis in a Poisson field of nodes of finite area," *IEEE Trans. Vehicular Technology*, vol. 58, pp. 1776–1783, May 2009.
- [4] M. Win, P. Pinto, and L. Shepp, "A mathematical theory of network interference and its applications," *Proc. IEEE*, vol. 97, pp. 205–230, February 2009.

- [5] M. Haenggi and Radha K. Ganti, *Interference in Large Wireless Networks*, Now Publishers, 2009.
- [6] F. Baccelli and B. Błaszczyszyn, *Stochastic Geometry and Wireless Networks, Volume I - Theory*, Now Publishers, 2009.
- [7] F. Baccelli and B. Błaszczyszyn, *Stochastic Geometry and Wireless Networks, Volume II - Applications*, Now Publishers, 2009.
- [8] P. Cardieri, "Modeling interference in wireless ad hoc networks," *IEEE Commun. Surveys and Tutorials*, vol. 12, pp. 551–572, Fourth Quarter 2010.
- [9] M. Franceschetti and R. Meester, *Random Networks for Communication*, Cambridge University Press, 2008.
- [10] D. Stoyan, W. Kendall, and J. Mecke, *Stochastic Geometry and Its Applications, 2nd ed.* Wiley, 1996.
- [11] R. K. Ganti, J. G. Andrews, and M. Haenggi, "High-SIR transmission capacity of wireless networks with general fading and node distribution," *IEEE Trans. Inform. Theory*, vol. 57, pp. 3100–3116, May 2011.
- [12] R. Giacomelli, R. K. Ganti, and M. Haenggi, "Outage probability of general ad hoc networks in the high-reliability regime," *IEEE/ACM Trans. Networking*, vol. 19, pp. 1151–1163, Aug. 2011.
- [13] A. A. Abu Dayya and N. C. Beaulieu, "Outage probabilities of cellular mobile radio systems with multiple Nakagami interferers," *IEEE Trans. Veh. Tech.*, vol. 40, pp. 757–768, Nov. 1991.
- [14] Q. T. Zhang, "Outage probability of cellular mobile radio in the presence of multiple Nakagami interferers with arbitrary fading parameters," *IEEE Trans. Veh. Tech.*, vol. 44, pp. 661–667, Aug. 1995.
- [15] C. Tellambura, "Cochannel interference computation for arbitrary Nakagami fading," *IEEE Trans. Veh. Tech.*, vol. 48, pp. 487–489, Mar. 1999.
- [16] M. S. Alouini, A. Abdi, and M. Kaveh, "Sum of Gamma variates and performance of wireless communication systems over Nakagami-fading channels," *IEEE Trans. Veh. Tech.*, vol. 50, pp. 1471–1480, Nov. 2001.
- [17] L. Li, P. Vigneron, C. Brown, M. Shi, and T. Kunz, "On designing bandwidth constrained mobile tactical networks for complex terrains," *IEEE Commun. Mag.*, pp. 188 – 194, Feb. 2012.
- [18] A. Hasan and J. G. Andrews, "The guard zone in wireless ad hoc networks," *IEEE Trans. Wireless Commun.*, vol. 6, pp. 897–906, March 2007.
- [19] M. Krunz, A. Muqattash, and S.-J. Lee, "Transmission power control in wireless ad hoc networks: challenges, solutions, and open issues," *IEEE Network*, vol. 18, pp. 8–14, Sept.-Oct. 2004.
- [20] B. Alawieh, Y. Zhang, C. Assi, and H. Moutfah, "Improving spatial reuse in multihop wireless networks – a survey," *IEEE Commun. Surveys and Tutorials*, vol. 11, pp. 71–91, Third Quarter 2009.
- [21] D. Torrieri, *Principles of Spread-Spectrum Communication Systems, 2nd ed.* Springer, 2011.
- [22] D. Torrieri, "Performance of direct-sequence systems with long pseudonoise sequences," *IEEE J. Selected Areas Commun.*, vol. 10, pp. 770–781, May 1992.
- [23] G. B. Arfken and H. J. Weber, *Mathematical Methods for Physicists*, 6th ed., Elsevier, 2005.
- [24] J. Pearson, "Computation of hypergeometric functions," Master's thesis, University of Oxford, Sept. 2009.

## ACKNOWLEDGEMENTS

The authors would like to thank Salvatore Talarico for his programming assistance and suggestions related to the Appendix.



award for sustained contributions to the field.

**Don Torrieri** is a research engineer and Fellow of the US Army Research Laboratory. His primary research interests are communication systems, adaptive arrays, and signal processing. He received the Ph. D. degree from the University of Maryland. He is the author of many articles and several books including *Principles of Spread-Spectrum Communication Systems*, 2nd ed. (Springer, 2011). He teaches graduate courses at Johns Hopkins University and has taught many short courses. In 2004, he received the Military Communications Conference achievement



**Matthew C. Valenti** is a Professor in Lane Department of Computer Science and Electrical Engineering at West Virginia University. He holds BS and Ph.D. degrees in Electrical Engineering from Virginia Tech and a MS in Electrical Engineering from the Johns Hopkins University. From 1992 to 1995 he was an electronics engineer at the US Naval Research Laboratory. He serves as an associate editor for *IEEE Wireless Communications Letters* and as Vice Chair of the Technical Program Committee for Globecom-2013. Previously, he has served as a track or symposium co-chair for VTC-Fall-2007, ICC-2009, Milcom-2010, ICC-2011, and Milcom-2012, and has served as an editor for *IEEE Transactions on Wireless Communications* and *IEEE Transactions on Vehicular Technology*. His research interests are in the areas of communication theory, error correction coding, applied information theory, wireless networks, simulation, and secure high-performance computing. His research is funded by the NSF and DoD. He is registered as a Professional Engineer in the State of West Virginia.